Oncogenic mutations in IDH1 affect the MUL1-mediated NF-κB pathway activation

Ya Gao[1], Maurice de Wit[1], Iris de Heer[1], Jory Prince[1], Eduard Struys[3], Cassandra Verheul[2], Gajja S. Salomons[3], Peter Sillevis Smitt[1], Martine Lamfers[2], Pim J. French[1]

Departments of [1] Neurology and [2] Neurosurgery, Erasmus Medical Center, Rotterdam, the Netherlands; [3] Department of Clinical Chemistry, VU University Medical Center, Amsterdam the Netherlands

Under revision

ABSTRACT

Background

The gene encoding isocitrate dehydrogenase 1 (*IDH1*) is frequently mutated in gliomas. *IDH1*^{R132H} is the most common mutation in *IDH1*, resulting in a neomorphic enzyme that produces D-2-hydroxyglutarate (D2HG). The elevated level of D2HG inhibits a number of pathways that ultimately causes cells to remain in an undifferentiated stem-like state. It is however unclear whether all pathways affected by mutant IDH1 have been identified.

Methods

We performed a biotin pull-down assay followed by mass spectrometry to identify potential binding partners of IDH1. The interaction was confirmed for both IDH1-wildtype (IDH1^{wt}) and IDH1-mutants (IDH^{R132H}, IDH1^{R132C} and IDH1^{G70D}) using western blot analysis and proximity ligation assays. An NF-kB luciferase reporter assay was used to determine NFKB pathway activation. Proliferation was measured using an IncuCyte (Essen bioscience).

Results

Our data show that IDH1^{R132H}, but not IDH1^{wt}, inhibited the TNFα-induced NF-κB pathway activation. We demonstrate that this inhibition was mediated by D2HG and was MUL1 dependent. In IDH1^{wt}-expressing cells, TNFα induces an immediate transient growth arrest. In contrast, IDH1^{R132H}-expressing cells continue to grow following stimulation with TNFα stimulation. We show that this reduced growth attenuation was also observed in IDH1^{wt}-expressing cells treated with octyl-D2HG and it was dependent on MUL1.

Conclusion

Our data indicate that IDH1 interacts with MUL1 and we show that IDH1 mutations inhibit the MUL1-mediated NF-κB pathway activation. This inhibition ultimately leads to an insensitivity to stimuli that inhibit cell growth.

INTRODUCTION

Somatic mutations in the *isocitrate dehydrogenase 1* (*IDH1*) gene have been identified in more than 70% of diffuse astrocytomas, oligodendrogliomas and secondary glioblastomas (sGBMs) (1-3). Mutations are almost always heterozygous and over 90% of these mutations are missense mutations leading to replacement of arginine 132 by histidine (R132H) within the catalytic domain ($IDH1^{R132H}$). Mutations in the IDH1 gene also occur in several other tumor types including acute myeloid leukemia, chondrosarcomas and intrahepatic cholangiocarcinomas (4-6). Wildtype IDH1 catalyzes the decarboxylation of isocitrate to α-ketoglutarate (αKG) and produces NADPH, whereas mutant IDH1 reduces αKG to generate D-2-hydroxyglutarate (D2HG) and produces $NADP^+$ (7). Mutations in the IDH1 gene are one of the earliest genetic aberrations during oncogenesis of gliomas, especially those of lower grade (lower grade glioma, LGG) (8). IDH1 mutations are clonal and retained as gliomas progress in time to a higher grade, suggesting continuous dependence on the mutation by tumor cells (3, 9). These properties make mutant IDH1 a good target for therapy.

The product of mutant IDH1, D2HG, shares structural resemblance with αKG and the elevated D2HG level interferes with a number of αKG-dependent enzymes (10). Examples include TET2 and KDM4A/JMJD2A, enzymes involved in the demethylation of DNA and histones (10-12). The increased level of D2HG also affects the hydroxylation of HIF-1α by the Egl nine homolog 1 (EGLN1) prolyl hydroxylase (13), which leads to an upregulation of HIF1α-inducible genes including vascular endothelial growth factor (VEGF) (14, 15). It should be noted that, due to the different affinities for D2HG, the αKG-dependent enzymes are affected at various levels (10, 12). As a result of the competitive inhibition of αKG-dependent oxygenases, IDH1 mutant cells ultimately remain in an undifferentiated state (16).

Although these studies demonstrate the involvement of mutant IDH1 and the concomitant increase in D2HG during oncogenesis, it is possible that other pathways are also affected by mutant IDH1 and D2HG. In this study, we performed a biotin-pull down and identified mitochondrial ubiquitin E3 ligase 1 (MUL1) as a novel binding partner for IDH1. We show that mutant IDH1 and the elevated D2HG level affects the function of MUL1 in regulating the NF-κB pathway.

MATERIALS AND METHODS

Constructs and cell lines

IDH1^{wildtype} and *IDH1*^{R132H} were cloned into pEGFP-C2 (Addgene) as described previously (17). Additional mutations were created using site-directed mutagenesis with primers (5'-CTATCATCATAGGTTGTCATGCTTATGGGGATCA ATAC-3' and 5'-CCATA AGCATGACA ACCTATGATGATAGGTTTTAC-3') for *IDH1*^{R132C} and (5'-AGA AGCATA ATGTTGACGTCA A ATGTGCCAC-3' and 5'-GTGGCACATTT-GACGTCA ACATTATGCTTCT-3') for *IDH1*^{G70D}. All the constructs were checked by Sanger sequencing. HEK and U87 cell lines stably expressing IDH1^{wt}, IDH1^{R132H} and eGFP were cultured in selective DMEM medium with 400 to 600 µg/ml Geneticin (Gibco, Invitrogen, Breda, the Netherlands) as described (18). The *MUL1* clone was a gift kindly provided by Dr. Bae (19). Patient-derived glioma stem cell line was cultured as previous (20). *IDH1* mutation status was confirmed using Sanger sequencing. The use of patient tumor tissue was approved by the Institutional Review Board of the Erasmus Medical Center, Rotterdam.

HEK MUL1 Knockout cells

5x 10^5 HEK cells were seeded in a well of a 6-well plate 24 hours before transfection. Transfection was performed using FuGENE (Promega, Leiden, The Netherlands) according to manufacturer's protocol with CRISPR/Cas9 constructs targeting the first exon of *MUL1* as described (21) and co-transfected using an eGFP reporter construct. Single cell sorting was applied to the transfected cells by a BD FACS Aria III (Beckton Dickinson, NJ, USA) based on GFP expression. Genotyping was performed when each clone reached about 90 % confluency in a 96-well plate.

Biotin pulldown and mass spectrometry

IDH1^{wt} and *eGFP* constructs were transfected into HEK cells using Polyethylenimine "Max" (Polysciences, Eppelheim, Germany). IDH1^{wt} protein was isolated using Dynabeads (Life Technologies, Carlsbad, USA) and proteins specifically bound to IDH1^{wt} were identified as described (18).

Proximity ligation assay (PLA)

HEK cells were seeded in 8-well LabTek glass slide plates (Thermo Fisher Scientific, Rochester, USA) and transfected with IDH1 constructs using FuGENE (Promega) according to manufacturer's protocol. Primary glioma cells were cultured as described (20) and transferred on glass slides by Cytospin™ (Thermo Scientific) at 300 rpm for 5 minutes at room temperature. Cells were fixed with 4 % PFA and permeablized with 10 % Triton X-100 in PBS for 10 minutes, followed by twice PBS/Tween wash.

The PLA assay was performed according to manufacturer's protocol (DUOlink, Uppsala, Sweden). Antibodies used were IDH1 (1:500, Sigma-Aldrich, Zwijndrecht, the Netherlands), eGFP (1:500, Abcam, Hilversum, The Netherlands) and MUL1 (1:500, Sigma-Aldrich).

Immunoblotting

Western blots were performed as previously described (22). Primary antibodies used were directed against IκB (1:1000, Cell Signaling), Mul1 (1:1000), IDH1 (1:1000), GFP (1:1000), β-actin (1:5000, Sigma-Aldrich), and HPRT (1:1000, Abcam). Intensity of proteins bands on the blots was quantified using Image Lab 5.1 (BIO-RAD).

Luciferase reporter assay

Cells were plated and transfected with the NF-κB reporter constructs (accession code EU581860, Promega) along with IDH1 mutant constructs and controls using FuGENE according to manufacturer's protocol. Cells were lysed in 100 µl lysis buffer followed by incubation with luciferin substrate (Promega). Luciferin unit was quantified by a Dual–Luciferase Reporter Assay System (Promega). Three independent experiments were performed.

Proliferation assay

Proliferation assays were performed using an IncuCyte (Essen Bioscience, Ann Arbor, MI) as described (22). $4x10^5$ cells were seeded in each well of a 96-well plate. Cells were stimulated with 1 µg/ml TNFα when they were at the log growth phase. Growth curves were constructed using the IncuCyte software based on data extracted from Confluency v1.5 metric. Confluency was measured every 2 hours. Growth rate was calculated using confluency at 3 sequential time points before and after TNFα stimulation divided by time (% confluency/ hours). This experiment was performed three times independently. Each experiment included 5 wells per condition as technical replicates. P values were calculated using Student's t-test with even variance.

RESULTS

IDH1 associates with MUL1

To identify binding partners for IDH1, we performed a biotin-pulldown using HEK cells stably expressing IDH1-wildtype ($IDH1^{wt}$) (18). Subsequent mass spectrometry identified over 90 candidates. We filtered out duplicate hits, proteins that also associated with the control construct (bio-eGFP) and proteins present in >10% of CRAPome pulldown results (23). Six candidate IDH1-interacting proteins remained

(Table 1). Although the Mascot score of all IDH1-interacting proteins was low compared to other studies performed in our laboratory (22), MUL1 showed the highest affinity for $IDH1^{wt}$. We therefore further investigated the potential interaction between these two proteins.

Table 1. Potential binding partners of $IDH1^{wt}$

Gene symbol	Mascot score	Description
MUL1	283	Mitochondrial ubiquitin ligase activator of NF-κB 1
FLOT1	194	Flotillin 1
SRP14	184	Signal recognition particle 14 kDa protein
OTUB1	176	Ubiquitin thioesterase OTUB1
CYR61	100	Uncharacterized protein
AAAS	87	Achalasia variant

To validate the mass spectrometry results, we performed an independent biotin pull-down using HEK cells stably expressing $IDH1^{wt}$, $IDH1^{R132H}$ and eGFP. Subsequent western blot confirmed the association between MUL1 and IDH1 (both $IDH1^{wt}$ and $IDH1^{R132H}$) but not in control cells expressing eGFP (Fig. 1A). This association was further confirmed using an *in situ* proximity ligation assay (PLA) in which a red fluorescent signal is only present when two proteins are in close proximity. In transiently transfected HEK cells, a strong signal was observed in cells expressing IDH1 ($IDH1^{wt}$ and $IDH1^{R132H}$) but not in eGFP controls (Fig. 1B). Two additional IDH1 mutation constructs were included in these experiments, $IDH1^{R132C}$ and $IDH1^{G70D}$. The $IDH1^{R132C}$ mutation has a higher enzymatic activity in producing D2HG than $IDH1^{R132H}$ (24) and $IDH1^{G70D}$ is a loss-of function mutation reported in 10 % of thyroid cancers (7, 25). Increased intracellular D2HG levels were indeed detected in HEK cells expressing $IDH1^{R132C}$ but not $IDH1^{G70D}$ (supplementary Fig. 1). Both $IDH1^{R132C}$ and $IDH1^{G70D}$ mutants also showed specific association with MUL1 (Fig. 1B). The association between IDH1 and MUL1 by PLA was further confirmed in U87 glioblastoma cell lines that stably expressed either $IDH1^{wt}$ or $IDH1^{R132H}$ (Fig. 1C). Moreover, the interaction was also detected in one primary cell lines derived from a $IDH1^{wildtype}$-GBM and two $IDH1^{R132H}$-mutated LGG (glioma stem cells, GCS) (Fig. 1D and E). PLA results were validated in three independent experiments. These experiments demonstrate that IDH1, both wildtype and mutant, interact with MUL1 and that the interaction is independent of the ability of IDH1 to produce D2HG.

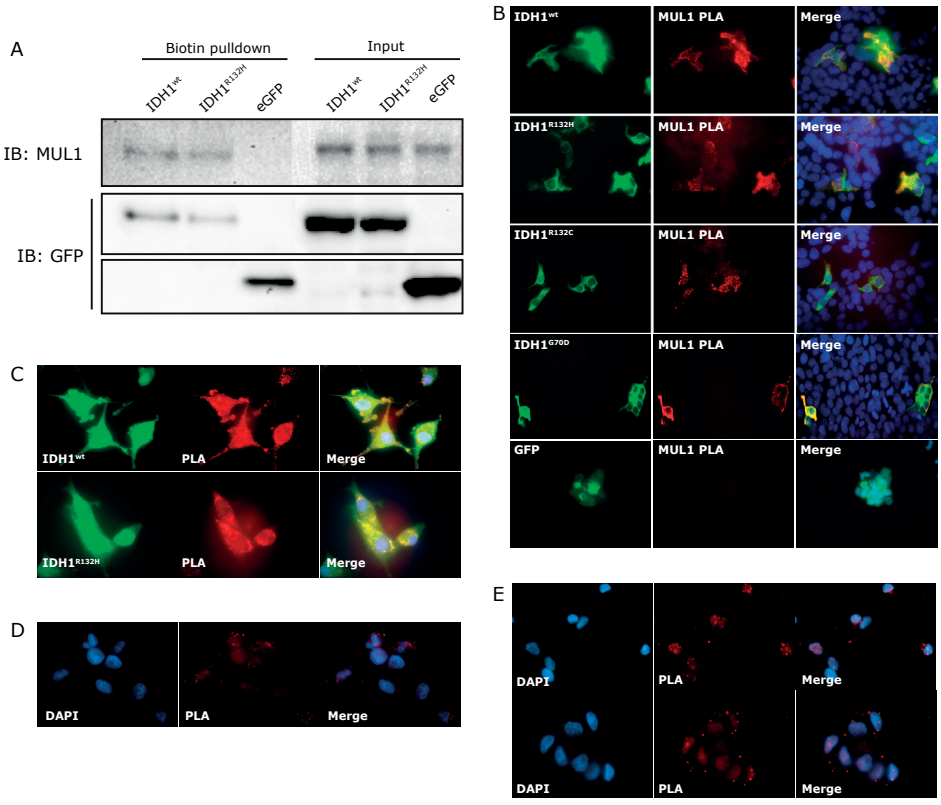

Figure 1. Association between MUL1 and IDH1. MUL1 protein was detected before and after biotin pull-down using HEK cells expressing IDH1 constructs (A). No MUL1 protein was associated with IDH1 in control eGFP-expressing cells. In PLA assays, a red fluorescent signal is seen when two proteins are in close proximity. Proximity ligation assays confirm that MUL1 co-localizes with IDH1 but not with eGFP controls. Results are shown for HEK cells (B) and U87 cells (C). Primary IDH1R132H mutant glioma cells confirmed the co-localization in glioma cells. In this case, the PLA was performed using IDH1 and MUL1 antibodies (D).

MUL1 is involved in the TNFα-induced activation of NF-κB pathway

MUL1 was initially identified as an activator of NF-κB pathway in a large-scale screen (26). However, luciferase reporter assays failed to show an activation of the NF-κB pathway by MUL1 overexpression (Supplementary Fig. 2). We therefore generated MUL1 knockout (MUL1 K.O.) HEK cells using CRISPR/Cas9 (Supplementary Fig. 3) and examined NF-κB pathway activation. Since IκB is degraded after activation of the canonical NF-κB pathway, we determined NF-κB pathway activation by measuring cellular IκB levels on western blot. As expected, western blot demonstrated a decreased IκB level in HEK cells upon TNFα stimulation (Fig. 2a and 2b). Interestingly, the IκB level was not affected when stimulating MUL1 K.O. cells with TNFα, which indicates that MUL1 plays an important role in the TNFα-induced activation of the NF-κB pathway.

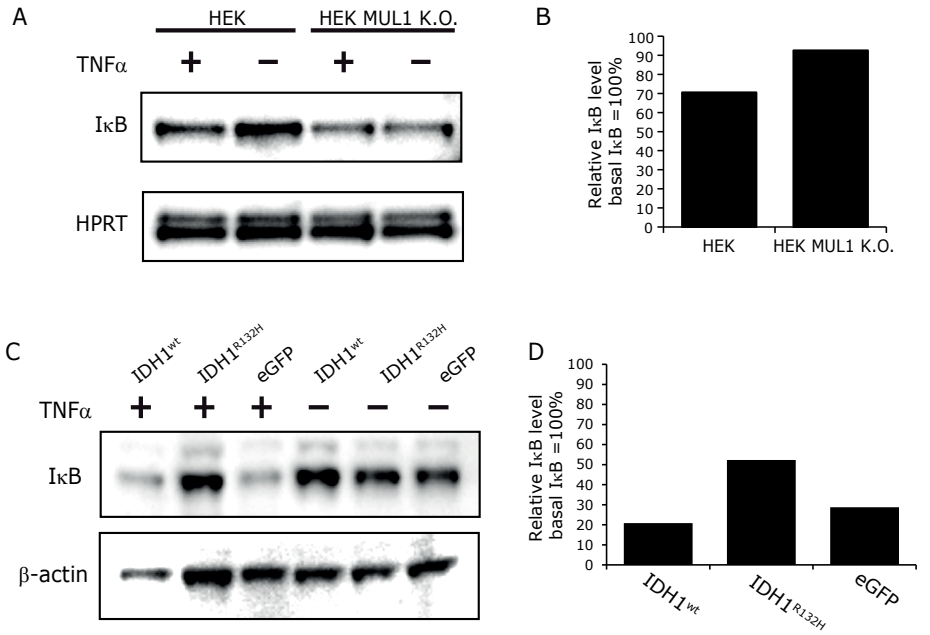

Figure 2. MUL1 depletion and IDH1 mutations results in insensitivity to TNFα stimulation. (A) Western blot showed that stimulation of HEK cells with TNFα results in a degradation of IκB in wildtype HEK cells. This degradation is absent in MUL1 K.O. cells. (B) quantification of protein bands in A. (C) IκB is degraded upon TNFα stimulation in HEK cells expressing IDH1wt but not cells expressing IDH1R132H. (D) Quantification of protein bands in B.

MUL1 is inhibited by D2HG-producing IDH1 mutants

We next measured the IκB levels upon TNFα stimulation in HEK cells stably expressing IDH1^{wt}, IDH1^{R132H} or eGFP (Fig. 2c and 2d). Similar to the eGFP control cells, TNFα induced a decrease in IκB levels in HEK cells expressing IDH1^{wt}. However, TNFα did not induce a decrease in IκB levels in HEK cells expressing IDH1^{R132H}. To determine whether the attenuated NF-κB pathway activation in IDH1^{R132H}-HEK cells was related to the elevated D2HG levels, we measured the IκB level in HEK cells in the presence of octyl-D2HG, a cell permeable analogue of D2HG (Fig. 3a and 3b). Similar to the HEK cells expressing IDH1^{R132H}, normal HEK cells cultured in the presence of octyl-D2HG showed less IκB degradation after TNFα stimulation. Our experiments therefore indicated that the TNFα-induced NF-κB pathway activation was inhibited by IDH1^{R132H} and D2HG.

To examine if NF-κB pathway activity is affected by D2HG in other cell types, we cultured human T lymphocytes in the presence of 300μM octyl-D2HG for 48 hours followed by stimulation with TNFα. Similar to observed in HEK cells, a reduced degradation of IκB was detected in the cells exposed to D2HG compared to cells exposed to PBS controls (Fig. 3c and 3d).

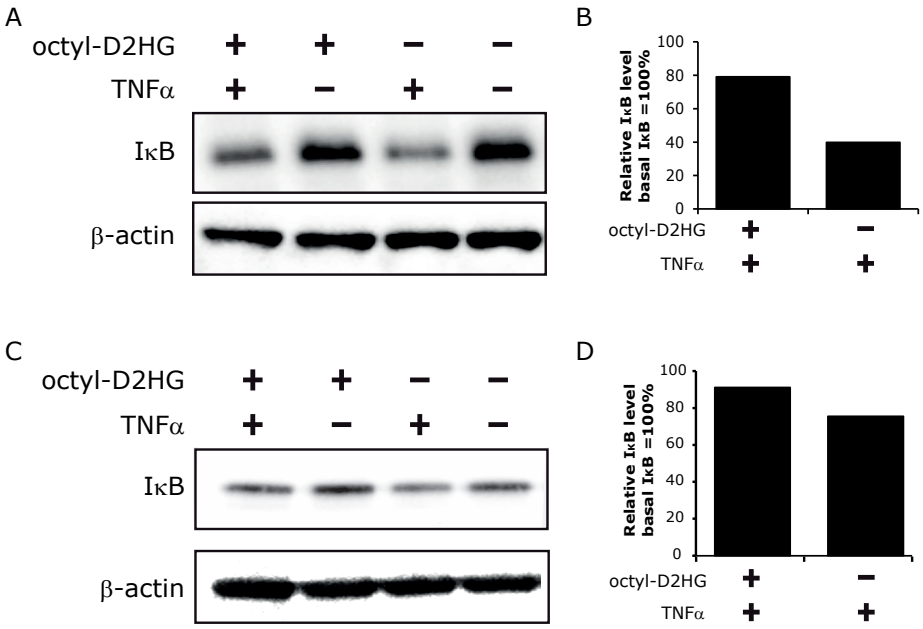

Figure 3. High levels of D-2HG result in insensitivity to TNFα stimulation. Western blot showing IκB degradation in HEK (A) and T lymphocytes (C) after stimulation with TNFα. This degradation is however reduced when cells are stimulated in the presence of 300μM octyl-D2HG. (B and D) Quantification of A and C respectively.

We next investigated NF-κB pathway activity using luciferase reporter constructs to validate our western blot data. For this, HEK cells stably expressing $IDH1^{wt}$, $IDH1^{R132H}$ or eGFP control were transfected with the NF-κB luciferase reporter construct (Fig. 4a). The basal level of NF-κB activity in HEK cells expressing eGFP control was similar to the HEK cells expressing $IDH1^{wt}$ ($n = 4$, $p = 0.314$). However, a lower NF-κB activity was detected in HEK cells expressing $IDH1^{R132H}$ ($n = 4$, $p = 0.007$). As observed in the western blot for IκB, our data showed that while TNFα stimulates the NF-κB pathway in $IDH1^{wt}$ and eGFP cells ($n = 4$, $p = 0.110$), the NF-κB pathway was less sensitive to TNFα stimulation in $IDH1^{R132H}$ cells ($n = 4$, $p = 0.020$). TNFα also resulted in less activation of the NF-κB pathway when normal HEK cells were cultured in the presence of 300 μM of octyl-D2HG (Fig. 4b, $p = 0.016$). These data therefore confirm that $IDH1^{R132H}$ and D2HG attenuate the TNFα-stimulated NF-κB pathway activity in HEK cells.

Cellular effects of IDH1 mutations on NF-κB pathway activation

To determine the cellular effect of IDH1 mutations on NF-κB pathway activation, we transfected HEK cells with various IDH1-mutation constructs and measured their growth rate before and after TNFα stimulation. HEK cells expressing $IDH1^{wt}$ and

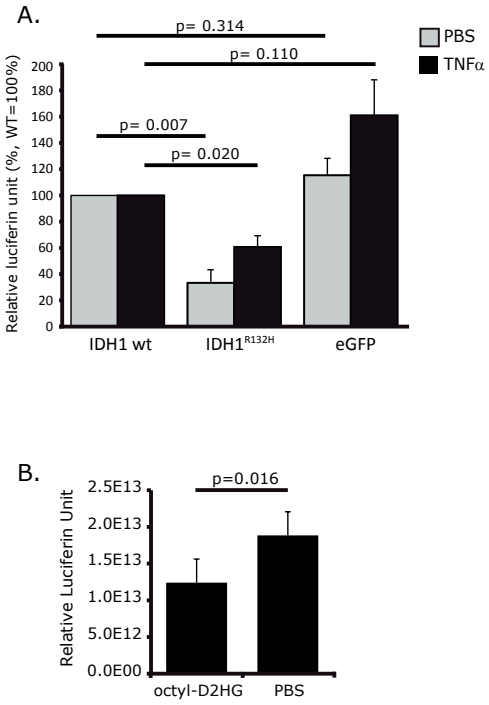

Figure 4. Luciferase reporter assays confirm the attenuated TNFα response in cells expressing IDH1R132H or incubated in the presence of D2HG. HEK cells expressing IDH1R132H showed less NF-κB activity compared to the controls at both basal and stimulated conditions (A). HEK cells treated with octyl-D2HG also showed less NF-κB activation compared to controls (B).

IDH1^{G70D} showed a temporary growth arrest after stimulation with TNFα (Fig. 5a and Supplementary Fig. 4a). IDH1^{wt} and IDH1^{G70D} cells grew at a rate of 1.0 % and 1.1 % confluency increase per hour respectively before TNFα stimulation (Supplementary Table 1). After TNFα stimulation, cells almost completely stopped growing and the growth rate reduced to 0.0 % and 0.1 % confluency increase per hour (100 % and 91 % reduction in growth rate). This decrease was highly significant, $p = 0.0004$ and $p = 0.0003$ for IDH1^{wt} and IDH1^{G70D} respectively. The TNFα induced growth arrest lasted for more than 10 hours in both IDH1^{wt} and IDH1^{G70D} cell lines.

Interestingly, HEK cells expressing IDH1^{R132H} or IDH1^{R132C} did not show the complete TNFα-induced growth attenuation (Fig. 5b and Supplementary Fig. 4b). Instead, the IDH1^{R132H} or IDH1^{R132C} cells remained growing albeit at reduced rate. Before TNFα stimulation, IDH1^{R132H} and IDH1^{R132C} cells grew at a rate that was similar to IDH1^{wt} and IDH1^{G70D} cells (1.1 % and 1.0 % confluency increase per hour respectively, Supplementary Table 2). After TNFα stimulation however, the rate was reduced to 0.3 % and 0.5 % confluency increase per hour, which was significantly higher than IDH1^{wt} and IDH1^{G70D} (Fig. 5c, $p = 0.0019$ for IDH1^{R132H} *v.* IDH1^{wt} and $p < 0.0001$ for IDH1^{R132C} *v.* IDH1^{wt}, $n = 5$). TNFα also was unable to induce a transient growth arrest in MUL1 K.O. cells (Fig. 5d-f and Supplementary Table 2). This growth arrest was independent

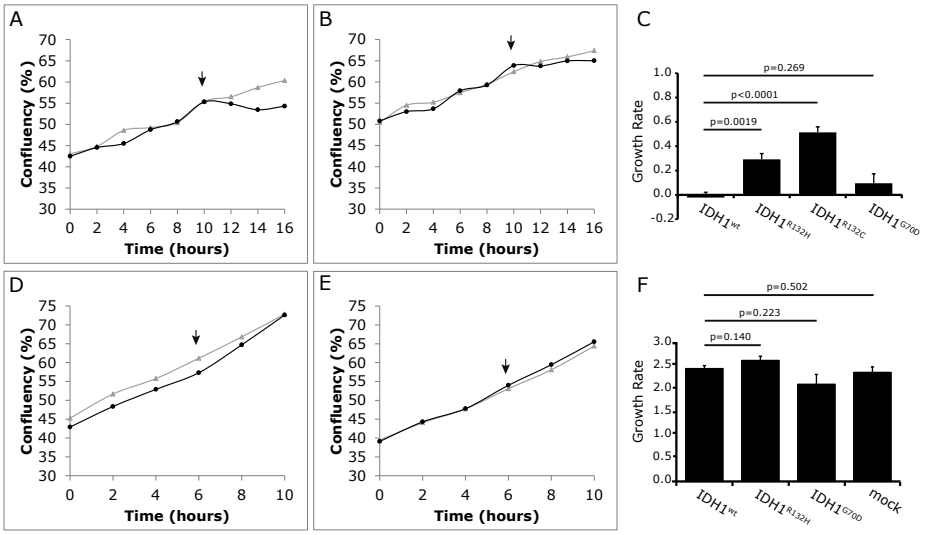

Figure 5. IDH1 mutant cells are insensitive to TNFα-induced growth arrest and this insensitivity is dependent on MUL1. Growth curves of HEK cells expressing IDH1wt (A) and IDH1R132H (B). As shown, the growth of HEK cells expressing IDH1wt was suspended following TNFα stimulation whereas HEK cells expressing IDH1R132H were less susceptible to TNFα–induced growth arrest. Growth rates of HEK cells stimulated with TNFα were calculated using confluency (%) divided by time (hours) (C). As expected, growth rates of HEK cells expressing IDH1wt and IDH1G70D after TNFα stimulation were similar and close to 0 (n=4, p=0.296). Whereas the growth rates of HEK cells expressing IDH1R132H and IDH1R132C were significantly higher than IDH1wt-expressing cells after TNFα stimulation (n=4, p=0.0019 and p<0.0001 respectively). Growth curves of HEK MUL1 K.O. cells expressing IDH1wt (D) and IDH1R132H (E). As can be seen, the growth of MUL1 K.O HEK cells does not change following TNFα stimulation, regardless of the presence of IDH1 mutations. The growth rates of HEK MUL1 K.O. cells expressing IDH1wt showed no difference compared to the HEK MUL1 K.O. cells expressing IDH1R132H or IDH1G70D after TNFα stimulation (F, all p values were not significant). Black lines: TNFα stimulation, grey lines: control. The arrow denotes the time point where cells were stimulated with TNFα.

of IDH1 expression as it was absent in MUL1 K.O. cells expressing either $IDH1^{wt}$, $IDH1^{R132H}$, $IDH1^{G70D}$ or mock control (Fig. 5d and f, Supplementary Fig. 4c and 4d and Supplementary Table 2). These results demonstrate that the impaired TNFα-induced growth arrest depends on expression of MUL1 and is inhibited by IDH1 mutants that produce D2HG.

DISCUSSION

In this study, our biotin-pull down assay identified MUL1 as a novel binding partner for IDH1. We show that mutant IDH1 and the elevated D2HG level affect the function of MUL1 in inhibiting the activation of the NF-κB pathway. This ultimately results in an attenuated TNFα-induced growth arrest of cells. Our study therefore identified

the NF-κB pathway as a pathway that is affected by oncogenic mutations in IDH1 and elevated levels of D2HG.

MUL1 was first identified to be an activator of the NF-κB pathway in a large-scale screen (26). Although our data failed to show activation of the NF-κB pathway by MUL1 overexpression, our data do show that MUL1 plays an important role in the TNFα-induced NF-κB pathway activation as this activation is absent in MUL1 K.O. cells (Fig. 5).

A previous study highlighted a potential tumor suppressor function of MUL1 as it showed significantly decreased expression level in several cancer cell lines compared to normal tissue (27). Moreover, the *MUL1* gene is homozygously deleted at a low but significant frequency in various cancer types including pancreatic cancers (7.3 %) and cholangiocarcinomas (3.4 %) (28). Our data are consistent with MUL1 functioning as a tumor suppressor gene as we show that MUL1 is involved in mediating growth arrest following TNFα stimulation and MUL1 K.O. cells do not show such growth arrest.

Our data show that MUL1 interacted with IDH1, regardless of the presence of oncogenic IDH1 mutants that produce D2HG (Fig. 2). A similar inhibition was observed in normal HEK cells treated with octyl-D2HG, which suggests that D2HG is a key mediator of the inhibition (Fig. 3). Similar to MUL1 K.O. cells, cells expressing $IDH1^{R132H}$ or $IDH1^{R132C}$ continued to grow following TNFα stimulation (Fig. 5b and Supplementary Fig. 4b). It should be noted that MUL1 K.O. cells were completely insensitive to TNFα induced growth inhibition whereas cells expressing $IDH1^{R132H}$ or $IDH1^{R132C}$ showed some arrest in their growth. It is possible that higher D2HG levels are required for a complete inhibition.

The mechanism behind the inhibitory effect of IDH1 on the TNFα-induced growth arrest remains to be elucidated. It is possible that, similar to other pathways affected by mutant IDH1, αKG-dependent enzymes are involved. Nevertheless, our study clearly demonstrates that mutant IDH1, and the concomitant increase in D2HG, are involved in regulating the NF-κB pathway. The clinical efficacy of inhibiting D2HG production in IDH1 mutated tumors is currently being investigated. Our data suggest that MUL1 is a downstream target for treatment in IDH mutated tumors and may be amenable for targeting.

Accumulated D2HG levels were detectable not only within IDH-mutated tumor cells but also in their extracellular environment (29, 30). It is possible that high extracellular D2HG levels result in elevated D2HG levels within stromal cells surrounding the

tumor (e.g. by passive diffusion or uptake). If D2HG reaches high enough concentrations, it could affect the function of those cells. The TNFα-induced NF-κB activation is critical for activating T lymphocytes and our data show that this activation was inhibited when culturing T lymphocytes in the presence of D2HG (31-33) (Fig. 3c). These data are in line with a study showing that D2HG decreased expansion of $CD4^+$ and $CD8^+$ T cells (30). Other studies have also shown a role for D2HG in affecting the immune system. For example, a recent study demonstrated that D2HG suppresses the number of T lymphocytes recruited to the LGGs by inhibiting CXCL10 expression (34).

In conclusion, our data indicated that IDH1 interacts with MUL1 and we show that IDH1 mutations inhibit the MUL1-mediated NF-κB pathway activation. This inhibition ultimately leads to an insensitivity to stimuli that inhibit cell growth.

REFERENCES

1. Balss J, Meyer J, Mueller W, Korshunov A, Hartmann C, von Deimling A. Analysis of the IDH1 codon 132 mutation in brain tumors. Acta Neuropathol. 2008 Dec;116(6):597-602.
2. Parsons DW, Jones S, Zhang X, Lin JC, Leary RJ, Angenendt P, et al. An integrated genomic analysis of human glioblastoma multiforme. Science. 2008 Sep 26;321(5897):1807-12.
3. Yan H, Parsons DW, Jin G, McLendon R, Rasheed BA, Yuan W, et al. IDH1 and IDH2 mutations in gliomas. N Engl J Med. 2009 Feb 19;360(8):765-73.
4. Mardis ER, Ding L, Dooling DJ, Larson DE, McLellan MD, Chen K, et al. Recurring mutations found by sequencing an acute myeloid leukemia genome. N Engl J Med. 2009 Sep 10;361(11):1058-66.
5. Borger DR, Tanabe KK, Fan KC, Lopez HU, Fantin VR, Straley KS, et al. Frequent mutation of isocitrate dehydrogenase (IDH)1 and IDH2 in cholangiocarcinoma identified through broad-based tumor genotyping. Oncologist. 2012;17(1):72-9.
6. Grassian AR, Pagliarini R, Chiang DY. Mutations of isocitrate dehydrogenase 1 and 2 in intrahepatic cholangiocarcinoma. Curr Opin Gastroenterol. 2014 May;30(3):295-302.
7. Dang L, White DW, Gross S, Bennett BD, Bittinger MA, Driggers EM, et al. Cancer-associated IDH1 mutations produce 2-hydroxyglutarate. Nature. 2009 Dec 10;462(7274):739-44.
8. Watanabe T, Nobusawa S, Kleihues P, Ohgaki H. IDH1 mutations are early events in the development of astrocytomas and oligodendrogliomas. Am J Pathol. 2009 Apr;174(4):1149-53.
9. Bai H, Harmanci AS, Erson-Omay EZ, Li J, Coskun S, Simon M, et al. Integrated genomic characterization of IDH1-mutant glioma malignant progression. Nat Genet. 2016 Jan;48(1):59-66.
10. Xu W, Yang H, Liu Y, Yang Y, Wang P, Kim SH, et al. Oncometabolite 2-hydroxyglutarate is a competitive inhibitor of alpha-ketoglutarate-dependent dioxygenases. Cancer Cell. 2011 Jan 18;19(1):17-30.
11. Figueroa ME, Abdel-Wahab O, Lu C, Ward PS, Patel J, Shih A, et al. Leukemic IDH1 and IDH2 mutations result in a hypermethylation phenotype, disrupt TET2 function, and impair hematopoietic differentiation. Cancer Cell. 2010 Dec 14;18(6):553-67.
12. Chowdhury R, Yeoh KK, Tian YM, Hillringhaus L, Bagg EA, Rose NR, et al. The oncometabolite 2-hydroxyglutarate inhibits histone lysine demethylases. Embo Rep. 2011 May;12(5):463-9.
13. Koivunen P, Lee S, Duncan CG, Lopez G, Lu G, Ramkissoon S, et al. Transformation by the (R)-enantiomer of 2-hydroxyglutarate linked to EGLN activation. Nature. 2012 Feb 15;483(7390):484-8.
14. Fu Y, Zheng S, Zheng Y, Huang R, An N, Liang A, et al. Glioma derived isocitrate dehydrogenase-2 mutations induced up-regulation of HIF-1alpha and beta-catenin signaling: possible impact on glioma cell metastasis and chemo-resistance. Int J Biochem Cell Biol. 2012 May;44(5):770-5.
15. Zhao S, Lin Y, Xu W, Jiang W, Zha Z, Wang P, et al. Glioma-derived mutations in IDH1 dominantly inhibit IDH1 catalytic activity and induce HIF-1alpha. Science. 2009 Apr 10;324(5924):261-5.
16. Lu C, Ward PS, Kapoor GS, Rohle D, Turcan S, Abdel-Wahab O, et al. IDH mutation impairs histone demethylation and results in a block to cell differentiation. Nature. 2012 Feb 15;483(7390):474-8.

17. Gravendeel LA, Kouwenhoven MC, Gevaert O, de Rooi JJ, Stubbs AP, Duijm JE, et al. Intrinsic gene expression profiles of gliomas are a better predictor of survival than histology. Cancer Res. 2009 Dec 01;69(23):9065-72.
18. Bralten LB, Kloosterhof NK, Balvers R, Sacchetti A, Lapre L, Lamfers M, et al. IDH1 R132H decreases proliferation of glioma cell lines in vitro and in vivo. Ann Neurol. 2011 Mar;69(3):455-63.
19. Bae S, Kim SY, Jung JH, Yoon Y, Cha HJ, Lee H, et al. Akt is negatively regulated by the MULAN E3 ligase. Cell Res. 2012 May;22(5):873-85.
20. Balvers RK, Kleijn A, Kloezeman JJ, French PJ, Kremer A, van den Bent MJ, et al. Serum-free culture success of glial tumors is related to specific molecular profiles and expression of extracellular matrix-associated gene modules. Neuro Oncol. 2013 Dec;15(12):1684-95.
21. Yun J, Puri R, Yang H, Lizzio MA, Wu C, Sheng ZH, et al. MUL1 acts in parallel to the PINK1/parkin pathway in regulating mitofusin and compensates for loss of PINK1/parkin. Elife. 2014 Jun 04;3:e01958.
22. Erdem-Eraslan L, Gao Y, Kloosterhof NK, Atlasi Y, Demmers J, Sacchetti A, et al. Mutation specific functions of EGFR result in a mutation-specific downstream pathway activation. Eur J Cancer. 2015 May;51(7):893-903.
23. Mellacheruvu D, Wright Z, Couzens AL, Lambert JP, St-Denis NA, Li T, et al. The CRAPome: a contaminant repository for affinity purification-mass spectrometry data. Nat Methods. 2013 Aug;10(8):730-6.
24. Pusch S, Schweizer L, Beck AC, Lehmler JM, Weissert S, Balss J, et al. D-2-Hydroxyglutarate producing neo-enzymatic activity inversely correlates with frequency of the type of isocitrate dehydrogenase 1 mutations found in glioma. Acta Neuropathol Commun. 2014 Feb 14;2:19.
25. Hemerly JP, Bastos AU, Cerutti JM. Identification of several novel non-p.R132 IDH1 variants in thyroid carcinomas. Eur J Endocrinol. 2010 Nov;163(5):747-55.
26. Matsuda A, Suzuki Y, Honda G, Muramatsu S, Matsuzaki O, Nagano Y, et al. Large-scale identification and characterization of human genes that activate NF-kappa B and MAPK signaling pathways. Oncogene. 2003 May 22;22(21):3307-18.
27. Zhang BC, Huang J, Li HL, Liu T, Wang YY, Waterman P, et al. GIDE is a mitochondrial E3 ubiquitin ligase that induces apoptosis and slows growth. Cell Res. 2008 Sep;18(9):900-10.
28. Cerami E, Gao J, Dogrusoz U, Gross BE, Sumer SO, Aksoy BA, et al. The cBio cancer genomics portal: an open platform for exploring multidimensional cancer genomics data. Cancer Discov. 2012 May;2(5):401-4.
29. Aref S, Kamel Areida el S, Abdel Aaal MF, Adam OM, El-Ghonemy MS, El-Baiomy MA, et al. Prevalence and Clinical Effect of IDH1 and IDH2 Mutations Among Cytogenetically Normal Acute Myeloid Leukemia Patients. Clin Lymphoma Myeloma Leuk. 2015 Sep;15(9):550-5.
30. Pickard AJ, Sohn AS, Bartenstein TF, He S, Zhang Y, Gallo JM. Intracerebral Distribution of the Oncometabolite d-2-Hydroxyglutarate in Mice Bearing Mutant Isocitrate Dehydrogenase Brain Tumors: Implications for Tumorigenesis. Front Oncol. 2016;6:211.
31. Boothby MR, Mora AL, Scherer DC, Brockman JA, Ballard DW. Perturbation of the T lymphocyte lineage in transgenic mice expressing a constitutive repressor of nuclear factor (NF)-kappaB. J Exp Med. 1997 Jun 02;185(11):1897-907.
32. Caamano J, Hunter CA. NF-kappaB family of transcription factors: central regulators of innate and adaptive immune functions. Clin Microbiol Rev. 2002 Jul;15(3):414-29.
33. Li Q, Verma IM. NF-kappaB regulation in the immune system. Nat Rev Immunol. 2002 Oct;2(10):725-34.

34. Kohanbash G, Carrera DA, Shrivastav S, Ahn BJ, Jahan N, Mazor T, et al. Isocitrate dehydrogenase mutations suppress STAT1 and CD8 + T cell accumulation in gliomas. J Clin Invest. 2017 Apr 03;127(4):1425-37.

Supplementary Table 1. Growth rate of HEK cells expressing different IDH1 constructs before and after TNFα stimulation.

	Before TNFα (± SE)	After TNFα (± SE)	**Reduced growth rate after stimulation with TNFα (%)**	Before PBS (± SE)	After PBS (± SE)	**Reduced growth rate after stimulation with PBS (%)**
IDH1^{wt}	1.0±0.094	0.0±0.043	**100**	1.1±0.153	1.0±0.119	**10**
IDH1^{R132H}	1.1±0.049	0.3±0.048	**73**	1.0±0.064	0.9±0.103	**10**
IDH1^{R132C}	1.0±0.111	0.5±0.045	**50**	1.2±0.068	1.1±0.120	**8**
IDH1^{G70D}	1.1±0.040	0.1±0.078	**91**	1.0±0.021	1.0±0.108	**0**

Supplementary Table 2. Growth rate of MUL1 Knockout HEK cells expressing different IDH1 constructs before and after TNFα stimulation.

	Before TNFα (± SE)	After TNFα (± SE)	**Reduced growth rate after stimulation with TNFα (%)**	Before PBS (± SE)	After PBS (± SE)	**Reduced growth rate after stimulation with PBS (%)**
IDH1^{wt}	2.4 ±0.092	2.5±0.066	**0**	1.9±0.141	2.3±0.213	**0**
IDH1^{R132H}	2.2±0.098	2.6±0.091	**0**	2.0±0.073	2.5±0.193	**0**
DH1^{G70D}	1.8±0.123	2.1±0.215	**0**	1.9±0.216	2.0±0.170	**0**
mock	2.1±0.043	2.4±0.119	**0**	1.9±0.044	2.3±0.161	**0**

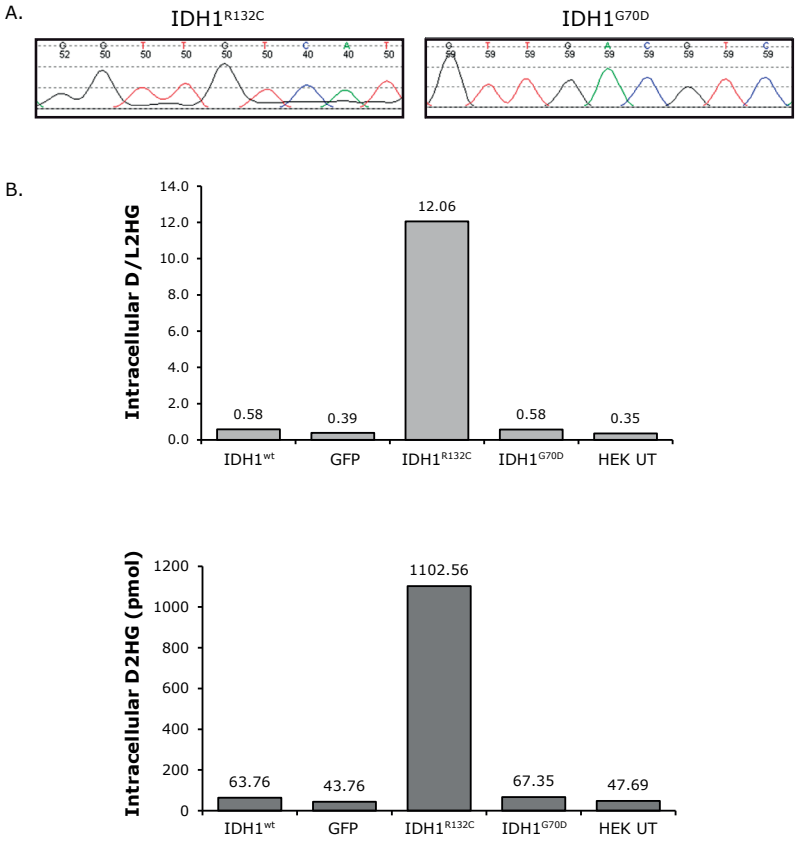

Supplementary Figure 1. Characterization of IDH1 constructs. Sanger sequencing confirmed the IDH1R132C and IDH1G70D (A). Elevated D2HG level was detected in HEK cells expressing IDH1R132C using LC/MS (B). The D2HG level was generalized using L2HG levels in each sample (upper panel). Absolute D2HG concentration of each sample is shown in the lower panel. UT: un-transfected.

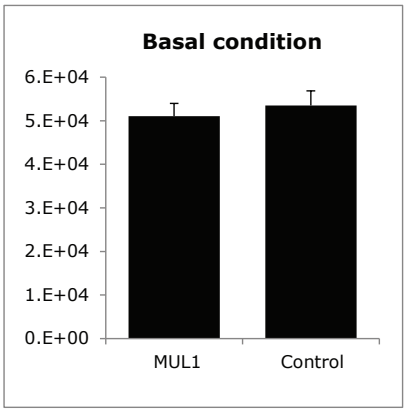

Supplementary Figure 2. Overexpression of MUL1 does not activate NF-κB pathway in HEK cells stably expressing eGFP.

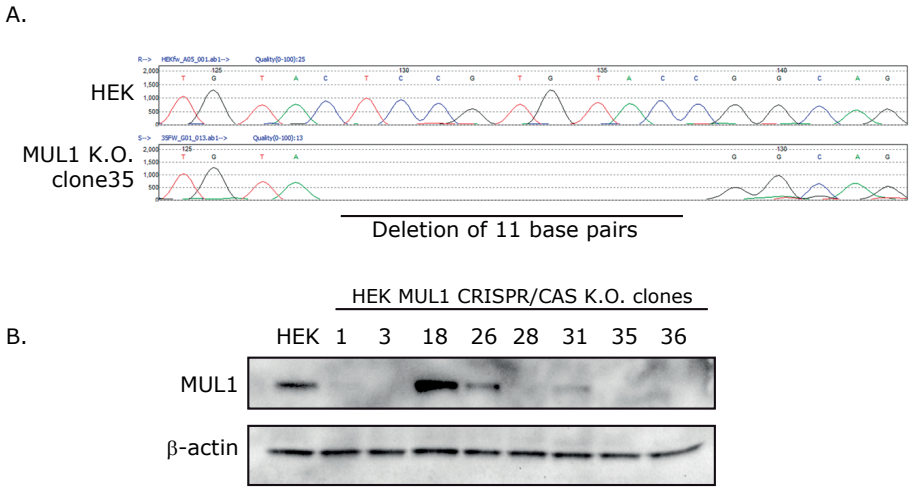

Supplementary Figure 3. Generation of MUL1 knockout (MUL1 K.O.) HEK cell lines using CRISPR/CAS9 system. A. Targeted Sanger sequencing showed 11 base pairs of deletion in the exon 1 of MUL1 in the MUL1 K.O. HEK cells. B. Immunoblotting confirmed the depletion of MUL1 in HEK K.O. cells.

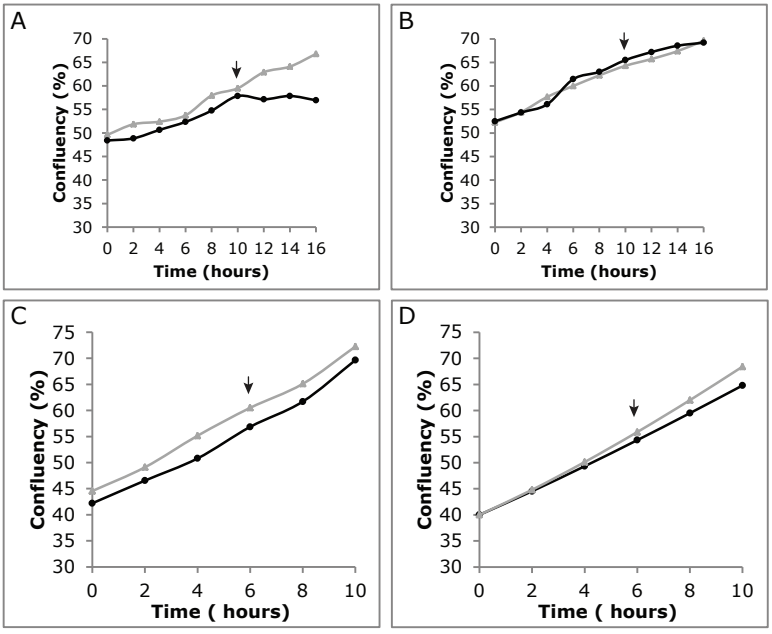

Supplementary Figure 4. TNFα-induced growth arrest is inhibited in IDH1R132C-expressing cells or MUL1 K.O. cells. Growth curves of HEK cells expressing IDH1G70D (A) and IDH1R132C (B). As shown, the growth of HEK cells expressing IDH1G70D was suspended following TNFα stimulation whereas HEK cells expressing IDH1R132C were less susceptible to TNFα–induced growth arrest. Growth curves of HEK MUL1 K.O. cells expressing IDH1G70D (C) and IDH1R132C (D). The growth of MUL1 K.O HEK cells does not change following TNFα stimulation, regardless of the presence of IDH1 mutations. Black lines: TNFα stimulation, grey lines: control. The arrow denotes the time point where cells were stimulated with TNFα.